

# TEMPLATE-BASED MULTIPLE HYPOTHESES TRACKING OF SMALL VESSELS

*Ola Friman, Milo Hindennach and Heinz-Otto Peitgen*

MeVis Research, Bremen, Germany

## ABSTRACT

A template tracking approach to the segmentation of small 3D vessel structures is presented. The main contributions are a general formulation of a vessel template function and a multiple hypotheses tracking framework that is shown to improve the tracking robustness. The methodology is demonstrated using CT angiography data of the liver to which a hybrid region growing and tracking segmentation is applied.

**Index Terms**— vessels, segmentation, tracking, template, multiple hypotheses, liver, arteries

## 1. INTRODUCTION

Computer aided vessel segmentation and vessel analysis are important tools in non-invasive CT and MRI angiography examinations. Most vessel segmentation algorithms currently in use are based on a growing process from a given start point; the differences between methods are generally found in the constraints imposed on the growing process. The simplest method is a region growing which connects voxels with similar image intensities. This approach works well for highly contrasted vessels but where the contrast is low the segmentation will leak into neighboring non-vessel tissue. To combat leakage, shape constraints and stronger vessel modeling must be introduced. A popular class of methods includes the front propagation or level-set techniques [1], in which the growing process is governed by a shape factor, e.g., the curvature of the growing front. This mitigates leakage problems and vessels with lower contrast may be segmented. Stronger vessel modeling can be implemented in a tracking framework. Tracking approaches identify vessels segment by segment and estimate vessel parameters such as the center line and radius as they go along. The tracking is commonly based on edge information in the image data, typically the second-order information in the Hessian matrix is utilized [2]. Explicit modeling of the vessel cross-section as an ellipse is also commonplace [3]. For smaller vessels ( $< 3$  voxels in diameter), there may not be enough data to fit a cross-section model and edge information may not be reliably estimated. An even stronger form of modeling is to describe the vessel locally as a linear tube segment [4, 5]. In this work, a tubular tracking algorithm based on a 3D vessel template is presented. The vessel template is an image patch containing an idealized vessel segment that is parameterized by the radius, center location and direc-

tion. Moreover, to traverse difficult vessel passages, such as bifurcations and areas of low contrast, a search tree is built to investigate different possible vessel paths.

## 2. VESSEL TEMPLATE

We target small low contrast vessels and therefore adopt a tubular model as discussed in the Introduction. The model is a template function  $T(\mathbf{x}; r, \mathbf{x}_0, \hat{\mathbf{v}}) : \mathbb{R}^n \rightarrow [0, 1]$  which maps a spatial coordinate  $\mathbf{x}$  to the interval  $[0, 1]$ . The template function is an idealized model of a local image neighborhood centered around the spatial center point  $\mathbf{x}_0$  through which a vessel with radius  $r$  is running in the direction of the unit vector  $\hat{\mathbf{v}}$ . To handle anisotropic voxels we track in a world coordinate system, i.e., the unit of the parameters is millimeters. The template has a circular cross-section, which is motivated by the fact that small vessels generally are round and that at small scales, the difference between a circular and an elliptic cross-section is negligible. The vessel template function is constructed as a composite function, i.e., as a function of a function. The two functions involved are described in detail below.

### 2.1. Vessel profile

The vessel profile models the image intensity variation along a line through the center of the vessel perpendicular to the vessel direction. The profile is a function  $p(d) : \mathbb{R} \rightarrow [0, 1]$  where  $d$  is the distance to the vessel center. A Gaussian profile has been used previously in the literature [6] and we use a similar function

$$p(d; r) = 2^{-\frac{d^2}{r^2}}. \quad (1)$$

Note that the profile function attains the value 0.5 for  $d = r$ , i.e., the Full Width Half Maximum (FWHM) of the function equals the diameter of the vessel.

### 2.2. Distance to a straight line

The second part of the template function is the minimum distance  $d$  from a point  $\mathbf{x} \in \mathbb{R}^n$  to a line running in the direction  $\hat{\mathbf{v}}$  through the point  $\mathbf{x}_0$ , see Fig. 1a. This distance is straightforwardly found via the Pythagorean theorem

$$\|\mathbf{x} - \mathbf{x}_0\|^2 = d^2 + \|\hat{\mathbf{v}}^T (\mathbf{x} - \mathbf{x}_0)\|^2 \quad (2)$$

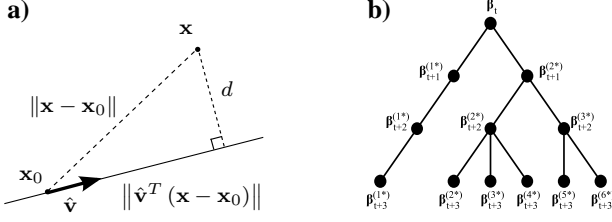


**Fig. 1.** **a)** Distance  $d$  from the point  $\mathbf{x}$  to the straight line running in direction  $\hat{\mathbf{v}}$  through the point  $\mathbf{x}_0$ . **b)** A search tree of depth 3 representing several possible vessel paths.

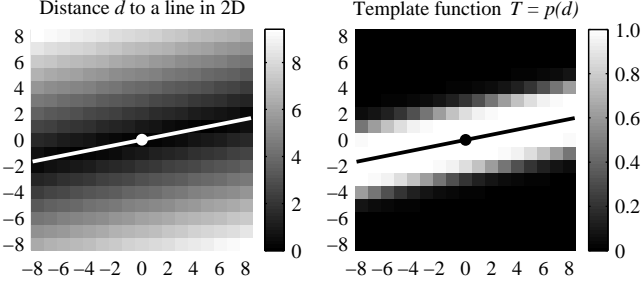


**Fig. 2.** The vessel template is generated by first calculating the distance to the line spanned by the template (left) and then applying a vessel profile function to this distance (right).

where  $\|\mathbf{x} - \mathbf{x}_0\|$  is the distance between  $\mathbf{x}$  and  $\mathbf{x}_0$ , and  $\hat{\mathbf{v}}^T (\mathbf{x} - \mathbf{x}_0)$  is the projection of the vector  $(\mathbf{x} - \mathbf{x}_0)$  onto the unit vector  $\hat{\mathbf{v}}$ . We now make the distance a function

$$d(\mathbf{x}; \mathbf{x}_0, \hat{\mathbf{v}}) = \sqrt{\|\mathbf{x} - \mathbf{x}_0\|^2 - \|\hat{\mathbf{v}}^T (\mathbf{x} - \mathbf{x}_0)\|^2} \quad (3)$$

parameterized by the center point  $\mathbf{x}_0$  and the direction  $\hat{\mathbf{v}}$ . Note that Eq. 3 is valid for any dimension, i.e., 2D, 3D, 4D etc.

### 2.3. The vessel template

The vessel template function is finally defined as the composite of the functions  $p(d; r)$  and  $d(\mathbf{x}; \mathbf{x}_0, \hat{\mathbf{v}})$

$$T(\mathbf{x}; r, \mathbf{x}_0, \hat{\mathbf{v}}) = p \circ d(\mathbf{x}) = p(d(\mathbf{x}; \mathbf{x}_0, \hat{\mathbf{v}}); r). \quad (4)$$

Hence, to calculate the template value for a spatial location  $\mathbf{x}$ , we first calculate the squared distance to the line spanned by the template center and the vessel direction. This distance is then mapped through the vessel profile function  $p(d; r)$ . Again, note that the vessel template function is general in that it can produce templates of arbitrary dimension. An example of a 2D vessel template generation is shown in Fig. 2.

### 2.4. Vessel template fitting

A local image neighborhood around a vessel template is modeled using a linear model, i.e., the voxel intensity  $I(\mathbf{x})$  at spa-

tial location  $\mathbf{x} \in \mathbb{R}^n$  is modeled as

$$I(\mathbf{x}) = k T(\mathbf{x}; r, \mathbf{x}_0, \hat{\mathbf{v}}) + m + \epsilon(\mathbf{x}), \quad (5)$$

where  $k$  is the vessel local contrast and  $m$  is the local mean image intensity level. The remaining term  $\epsilon(\mathbf{x})$  represents noise and interfering surrounding structures. To localize the fit of the vessel template to the image data, a Gaussian weight function centered over  $\mathbf{x}_0$  and with a width depending on the vessel radius is used. The image voxels with a non-negligible weight (e.g.,  $> 0.05$ ) are denoted by  $\mathbf{x}_i, i = 1 \dots n$ . The best template fit is defined as the solution to the following weighted least squared problem:

$$\min_{r, \mathbf{x}_0, \hat{\mathbf{v}}, k, m} \|\mathbf{W}(r, \mathbf{x}_0) [k \mathbf{T}(r, \mathbf{x}_0, \hat{\mathbf{v}}) + m - \mathbf{I}]\|^2, \quad (6)$$

where  $\mathbf{I}$  and  $\mathbf{T}(r, \mathbf{x}_0, \hat{\mathbf{v}})$  are  $(n \times 1)$  vectors containing the image data and template values for the spatial locations  $\mathbf{x}_i, i = 1 \dots n$ .  $\mathbf{W}(r, \mathbf{x}_0)$  is a diagonal matrix with the corresponding weights. We note that the least squares problem in Eq. 6 is linear in the image parameters  $k$  and  $m$  but nonlinear in the vessel parameters  $r, \mathbf{x}_0$  and  $\hat{\mathbf{v}}$ . This is known as a separable nonlinear least squares problem and a solution can be found by an iteration where the linear parameters are solved for while the nonlinear parameters are kept constant and vice versa [7]. The derivatives of the template function  $T(\mathbf{x}; r, \mathbf{x}_0, \hat{\mathbf{v}})$  with respect to translation, rotation and a radius change are required for the optimization. These are straightforwardly calculated but left out here due to space limitations.

### 2.5. Vessel template significance

A relevant question is whether the image data supports the hypothesis of the existence of a vessel with radius  $r$  at spatial location  $\mathbf{x}_0$  running in direction  $\hat{\mathbf{v}}$ ? To test this hypothesis, we investigate if the vessel contrast  $k$  is significantly different from zero. The classical way of doing this is to calculate a  $t$ -statistic  $t = \frac{k}{\text{std}(k)}$  where  $\text{std}(k)$  is the standard error, i.e., the square root of the variance, of the estimator of  $k$ . To calculate the standard error, we first define the  $(n \times 2)$  matrix  $\mathbf{X} = [T(\mathbf{x}_i; r, \mathbf{x}_0, \hat{\mathbf{v}}) \quad \mathbf{1}_n], i = 1 \dots n$  used for estimating the linear parameters  $k$  and  $m$ . Next, we introduce the contrast vector  $\mathbf{c} = [1, 0]^T$ , indicating that  $k$  is associated with the first column of  $\mathbf{X}$ . The standard error of the vessel contrast estimate is then obtained as

$$\text{std}(k) = \sqrt{\sigma^2 \mathbf{c}^T (\mathbf{X}^T \mathbf{W}^2 \mathbf{X})^{-1} \mathbf{X}^T \mathbf{W}^4 \mathbf{X} (\mathbf{X}^T \mathbf{W}^2 \mathbf{X})^{-1} \mathbf{c}} \quad (7)$$

where  $\mathbf{W}$  is the weight matrix used in Eq. 6 and  $\sigma^2$  is the estimate variance of the residual noise ( $\epsilon$  in Eq. 5). When  $\epsilon$  is Gaussian distributed, the  $t$ -statistic has an approximate standardized Gaussian distribution and a  $t$ -threshold of around 3 to 4 is therefore suitable. For real data, the threshold should be put somewhat higher, e.g., between 5 and 8.

### 3. VESSEL TRACKING

The tracking algorithm presented in this section is independent of the particular vessel model, i.e., it can be used with the vessel template in the previous section, an elliptical cross section model [3], superellipsoids [4] etc., as long as the model contains a spatial center point  $\mathbf{x}_0$ , a direction indicated by a unit vector  $\hat{\mathbf{v}}$  and a local vessel radius  $r$ . These vessel parameters are in this section collectively denoted by  $\beta = \{r, \mathbf{x}_0, \hat{\mathbf{v}}\}$ . The aim of the tracking procedure is to create a train of linear vessel segments  $\beta_0 \rightarrow \beta_1 \rightarrow \beta_2 \rightarrow \dots$  that describes the centerline and radius of the vessel. The process of going from  $\beta_t$  to  $\beta_{t+1}$  typically involves a prediction and a fit to the image data. In addition, a score function measuring the goodness of fit to the image data is required. This score is used to compare models and as a termination criterion.

The prediction of the next vessel segment  $\beta_{t+1}$  is found as a linear extrapolation from the center point  $\mathbf{x}_0$  in the direction  $\hat{\mathbf{v}}$  of the current vessel segment  $\beta_t$ . The linear prediction will not be exact for curved vessels but the ensuing fitting step can in general provide a proper correction. However, one must also consider the possibility that the vessel may branch and continue in two different directions. To capture a potential branching, a range of predictions must be evaluated. In this work, a systematic scan or sampling of the area in front of the current vessel segment is used. Formally, a collection of possible vessel continuations  $\beta_{t+1}^{(i)}, i = 1, 2, \dots$  from the current vessel segment  $\beta_t$  is generated. These predictions are placed evenly on the circle (2D) or sphere (3D) defined by a  $\pm\alpha$  degrees deviation from the current vessel direction  $\hat{\mathbf{v}}$ . All other vessel and image parameters, e.g., the radius and the vessel contrast, are kept constant in the prediction step. Each prediction has an associated score which serves as a basis for the further selection and processing. For the vessel template model, we use the  $t$ -statistic defined in Section 2.5 as score. Next, the best predictions are fitted to the image data, as described in Section 2.4 for the vessel template model. A suitable spacing between the generated predictions is around 15 degrees and the step length is in this work taken to be 1.5 times the current radius. A detailed discussion on the choice of step length can be found in [5].

Due to noise, artifacts and model imperfections, the locally best prediction is not guaranteed to give the globally best vessel path. In addition, at branchings two or more predictions will approximate the correct paths. To address this problem, multiple predictions or hypotheses are tracked. To select which predictions to pursue, the score pattern of the predictions is investigated, see Fig. 3. The score pattern will normally contain one maximum that lies close to the true vessel trajectory. At bifurcations, however, there will be one local maxima for each branch. Multiple local maxima may also occur in problematic regions where the exact vessel path is unclear. Therefore, to improve the tracking performance, all local maxima predictions are taken as hypotheses of the vessel path. This procedure is further elucidated with an ex-

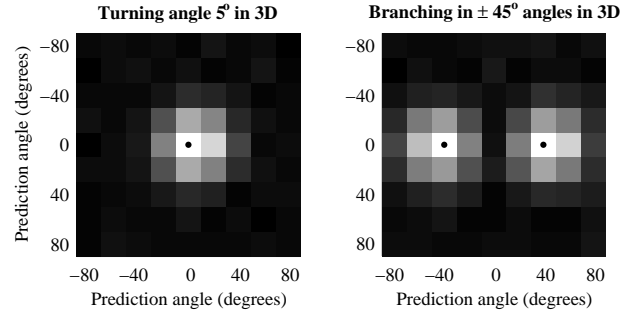


**Fig. 3.** Example score patterns of predictions of the next step. The maxima of these patterns, indicated with the dots, are taken as possible vessel paths to pursue.

ample, see Fig. 1b. Assume that the current vessel segment is parameterized by  $\beta_t$ . The generated predictions exhibit two local score maxima,  $\beta_{t+1}^{(1^*)}$  and  $\beta_{t+1}^{(2^*)}$ . Instead of immediately choosing one prediction to pursue, we continue the tracking from both predictions. A new prediction from  $\beta_{t+1}^{(1^*)}$  gives only one maximum,  $\beta_{t+2}^{(1^*)}$ , whereas the predictions from  $\beta_{t+1}^{(2^*)}$  again gives two maxima:  $\beta_{t+2}^{(2^*)}$  and  $\beta_{t+2}^{(3^*)}$ . Yet another round of predictions yields the maxima  $\beta_{t+3}^{(j^*)}, j = 1 \dots 6$ . Each of these predictions represents a possible vessel trajectory from  $\beta_t$ . By recursively tracking several trajectory hypotheses, a search tree is built. The depth of the tracking tree is herein denoted the search depth. When we have reached the pre-determined search depth, we decide where to go from  $\beta_t$ . This is done as follows: the average score along the tree path leading to each tree leaf  $\beta_{t+3}^{(j^*)}, j = 1 \dots 6$  is calculated. Among the leaves that survive a pre-determined score threshold, a branching check is performed as described further below. If no branching is detected, a step is taken from  $\beta_t$  towards the leaf with highest average score. If a branching is detected, steps are taken towards the leaves with highest average scores in each branch. If no leaves survive a pre-determined threshold, the tracking is terminated.

A branching detection is implemented as a clustering of the spatial center coordinates of the leaves of the search tree, cf. Fig. 1b. If the clustering results in two well defined clusters the tracking has passed a branching.

### 4. RESULTS

As a first experiment the effect of the tracking search depth is investigated. To this end, the vessel tracking algorithm is used to segment a 2D spiral with a radius of 1.5 pixels embedded in a  $256 \times 256$  Gaussian noise image, see Fig. 4. The maximum intensity of the spiral is 1 and the variance of the Gaussian noise is 1.0. An isotropic Gaussian smoothing matching the diameter of the spiral, i.e., with an FWHM of 3 pixels, was applied as pre-processing. The tracking was then applied

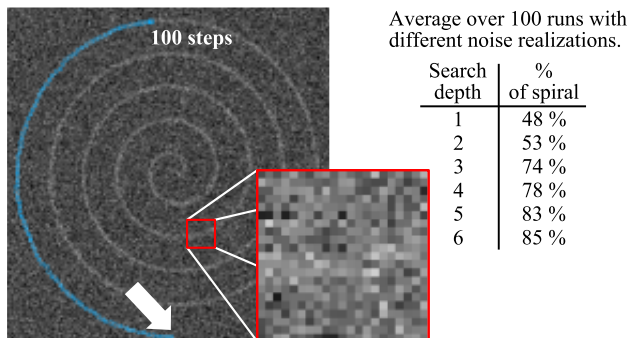


**Fig. 4. Image:** Spiral and 100 steps generated with the tracking algorithm. **Table:** Average percentage of the spiral that the tracking is able to segment with different search depths.

with search depths from 1 to 6 and with a  $t$ -score threshold of 3. A start point was given at the outer end of the spiral and the spiral tracking was repeated 100 times with different noise realizations. For each realization, the percentage of the spiral that the tracking was able to segment was recorded, see table in Fig. 4. The tracking performance increases dramatically with increased search depth, from 48% with search depth 1 to 85% with search depth 6. This demonstrates the improved segmentation robustness offered by tracking multiple hypotheses.

In liver surgery planning, the liver arteries play an important role in determining optimal resections and in predicting blood supply to remaining liver tissue. A problem is that the liver arteries are small and poorly contrasted in 3D CT angiography data. Presently, at our institute, the liver arterial system is segmented by hand on a daily basis, a procedure that takes 30-45 minutes for a trained expert. A goal of the proposed tracking procedure is to facilitate this process. A segmentation example of a  $512 \times 512 \times 401$  3D CT angiography volume is shown in Fig. 5, where a region growing was first applied to find the initial high-contrast part of the arterial tree (yellow vessels) and the proposed tracking algorithm was then automatically initiated at the region growing end points to track the low-contrast distal parts (red vessels). A search depth of 4 was used and the tracking takes about 3 seconds. Two branches that were not found by the region growing were initiated manually for the tracking algorithm (green vessels). This example illustrates how the tracking algorithm can be used with other vessel segmentation methods and how it can be used both for automatic as well as for semi-automatic segmentation.

## 5. DISCUSSION

Template matching and tracking are a well-known concepts in the computer vision community. One of the contributions in this paper is the general formulation of a vessel template function parameterized by the radius, direction and center point. Another contribution is the search tree for vessel tracking,

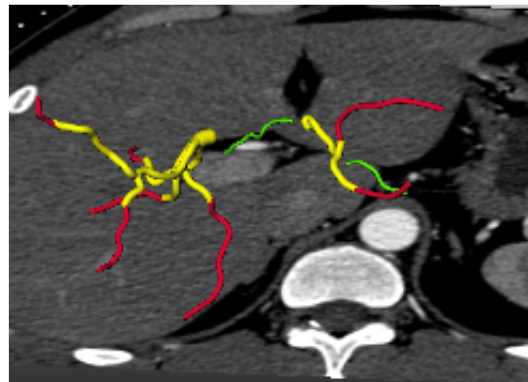


**Fig. 5.** Segmentation of the liver arteries. Yellow vessels were found with a region growing. Red and green vessels were found with the proposed tracking algorithm (automatic and manual seeding respectively).

which has been shown to increase the performance robustness. Tracking multiple hypotheses may be seen as a way around the unimodal restriction in the linear Kalman tracking framework. Another way to overcome this limitation is to employ so-called Particle Filtering, which recently has been used for vessel tracking [3]. Whereas the Particle Filter relies on stochastic predictions of the next tracking step, the tracking proposed here employs a systematic placement of the predictions (cf. Section 3) which reduces the computational burden.

## 6. REFERENCES

- [1] T. Deschamps and L. Cohen, “Fast extraction of tubular and tree 3D surfaces with front propagation methods,” in *ICPR’02*, 2002.
- [2] S. Aylward and E. Bullitt, “Initialization, noise, singularities, and scale in height ridge traversal for tubular object centerline extraction,” *IEEE Trans. Med. Imag.*, vol. 21, no. 2, pp. 61–75, 2002.
- [3] C. Florin et al., “Particle filters, a quasi-Monte Carlo solution for segmentation of coronaries,” in *MICCAI’05*, 2005, pp. 246–253.
- [4] J. Tyrrell et al., “Robust 3-D modeling of vasculature imagery using superellipsoids,” *IEEE Trans. Med. Imag.*, vol. 26, no. 2, pp. 223–237, 2007.
- [5] J. Lee et al., “Automatic segmentation of 3D micro-CT coronary vascular images,” *Med. Image Anal.*, vol. 11, no. 6, pp. 630–647, 2007.
- [6] K. Krissian et al., “Model based detection of tubular structures in 3D images,” *Comput. Vis. Image Underst.*, vol. 80, no. 2, pp. 130–171, 2000.
- [7] Å. Björck, *Numerical Methods for Least Squares Problems*, SIAM, 1996.